Analysis of Supercooled Liquid Water Measurements Using Microwave Radiometer and Vibrating Wire Devices

GEOFFREY E. HILL

Atek Data Corporation, Boulder, Colorado

(Manuscript received 19 October 1992, in final form 7 November 1993)

ABSTRACT

A review is made of the theoretical basis for using a vibrating wire to measure supercooled liquid water in clouds. The device consists of a vibrating wire and associated electronics added to radiosondes. The sensing wire that collects supercooled liquid water as rime ice is placed in a specially designed duct to minimize effects from swinging of the balloon as it ascends. Profiles of supercooled liquid water are vertically integrated, so that comparisons with radiometer measurements may be made. Because the radiometer senses all liquid whether from supercooled water, melting snow, or rain, any comparisons are valid only when the entire viewing path of the radiometer remains below 0°C.

Comparisons of supercooled liquid water measurements by the vibrating wire and a microwave radiometer show that the two methods are in good agreement. Even better agreement is obtained when the effect of a variable cloud radiation temperature on the radiometer measurement is taken into account. The remaining differences between the two measuring systems are attributed primarily to the different viewing paths, vertical for the radiometer and the balloon path for the vibrating wire.

These results along with previous laboratory calibrations of the vibrating wire lead to the conclusion that the vibrating wire sensor included in radiosondes is suitable to obtain vertical (balloon path) profiles of supercooled liquid water. It is also concluded that use of the radiosonde device and a microwave radiometer is a powerful combination for obtaining and analyzing data on supercooled liquid water.

1. Introduction

A large amount of supercooled liquid water (SLW) data has been collected using aircraft-carried instruments, such as the Johnson–Williams hot-wire device (Neel and Steinmetz 1952; Neel 1955), the Commonwealth Scientific and Industrial Research Organization (CSIRO) liquid water probe (King et al. 1981), and the Particle Measuring Systems probes (Knollenberg 1970, 1972). Use of aircraft is advantageous for obtaining spatial distributions of SLW; disadvantages are the flight preparation time, cost, and operational restrictions; the latter factor is particularly significant when measuring complete vertical profiles of SLW.

The introduction of the National Oceanic and Atmospheric Administration (NOAA) dual-frequency microwave radiometer developed at the NOAA Wave Propagation Laboratory (Guiraud et al. 1979; Snider et al. 1980; Hogg et al. 1983) has greatly facilitated measurement of the temporal distribution of liquid water. This capability is a major advantage of the microwave radiometer. For the radiometer to measure SLW unequivocally, the atmosphere viewed by the radiometer must be totally subfreezing; the radiometer cannot distinguish whether liquid water is warmer than 0°C or is supercooled. This fact is an important limitation of the radiometer when used to detect SLW. Another limitation is that the vertical distribution of SLW is not measured by this instrument.

A radiosonde device for measuring SLW (Hill and Woffinden 1980) consists of an exposed wire vibrating at its natural frequency. As SLW impinges on the wire, rime ice is formed and the natural frequency of vibration is reduced in accordance with the amount of ice collected. While this instrument does not have the capability of a radiometer to produce temporally continuous readings of SLW, it does have the capability of yielding vertical profiles.

The purpose of this article is to show that this radiosonde-carried device may be used to obtain measurements of SLW as a function of pressure or height (along the radiosonde path). The primary effort in this study is based upon comparisons of radiosonde soundings with the SLW device added and path-integrated SLW measured by microwave radiometry.

2. Vibrating wire sensor

a. Review of theory

The theoretical basis and the mechanical operation of the vibrating wire have been presented in detail by Hill and Woffinden (1980). A review of the theory is

Corresponding author address: Dr. Geoffrey E. Hill, Atek Data Corporation, 2300 Canyon Boulevard, Boulder, CO 80302.

presented herein. In addition, some simplifications to the original development are also presented. Instead of using equivalent sections of ice to represent the ice wire combination, as was done previously, the ice and wire segments (as shown in Fig. 1) are treated individually. Here, L_0 is the wire length and L_1 is a distance from the fixed end of the wire. Ice accumulates on the wire between L_0 and L_1; no ice accumulates between the fixed end of the wire and L_1, because that part of the wire is shielded from the airflow by a drive coil.

The natural vibration frequency of the activated wire and ice load can be found by equating the maximum potential (PE) and kinetic (KE) energies integrated along the wire length. In this treatment, the integration is done for the wire and ice as two terms. That is,

$$\mathrm{PE} = \int_0^{L_0} \frac{E_s I_s}{2}\left(\frac{\partial^2 y}{\partial x^2}\right)^2 dx + \int_{L_1}^{L_0} \frac{E_i I_i}{2}\left(\frac{\partial^2 y}{\partial x^2}\right)^2 dx, \quad (1)$$

$$\mathrm{KE} = \int_0^{L_0} \frac{M_s}{2}\left(\frac{\partial y}{\partial t}\right)^2 dx + \int_{L_1}^{L_0} \frac{M_i}{2}\left(\frac{\partial y}{\partial t}\right)^2 dx, \quad (2)$$

where y is the displacement from a stationary wire, x is the distance from the fixed end of the wire, and $M_{s,i}$ denote the masses per unit length for steel and ice, respectively. Here, M_s is 0.2025/8.9 (g cm^{-1}) and M_i is $\alpha D \rho_i$, where α is the ice thickness expressed as the number of wire diameters D, and ρ_i is the ice density. Parameters I_s and I_i are the area moments of inertia: $I_s = (\pi/64)D$ and $I_i = (\alpha^3/3 + \alpha^2/2 + \alpha/4)D^4$. The wire is steel piano wire with a Young's modulus $E_s = 2.0 \times 10^{12}$ dyn cm^{-2} and a diameter $D = 0.06$ cm; E_i is Young's modulus of ice, which is a strong function of ice density (Mellor 1983).

As before, an admissible function for the displacement from a stationary wire as a function of x and t is assumed as

$$y = B\left[\cos\left(\frac{\pi x}{2L_0}\right) - 1\right]\cos(\omega t), \quad (3)$$

where B is an unspecified amplitude. (In practice, B is about 1.25 cm.) Here, $\omega = 2\pi f$, and f is the vibration frequency. When (3) is used in (1) and (2) and then the two energy forms equated to each other (with $\sin\omega t$ and $\cos\omega t$ set equal to unity for maximum energy), the result is

$$f^2 = \frac{\pi^2 E_s (I_s + 0.4734 I_i/\beta)}{128 L_0^4 (0.2268 M_s + 0.2264 M_i)}, \quad (4)$$

where β is E_s/E_i. This result is equivalent to the earlier model (except for a change in the wire length), but the present derivation and presentation is substantially more straightforward.

As β approaches infinity the effect of ice stiffness is negligible. Ice stiffness effects at a temperature of

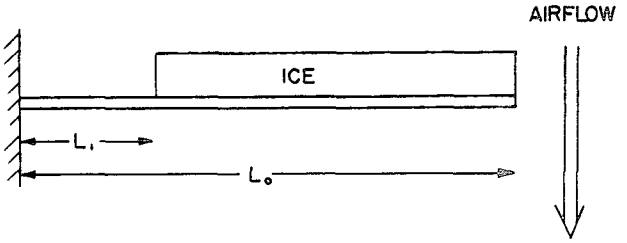

FIG. 1. Illustration of wire and ice load.

−14°C have been discussed in detail by Hill and Woffinden (1980). It was found that even with very large values of α ($\alpha = 15$), there was no evidence of any effect of ice stiffness on the relationship between the rate of change of frequency and supercooled liquid water concentration (SLWC). Further analysis of laboratory data contained in the research by Hill (1989) show that the effect of ice stiffness is negligible at temperatures as warm as −5°C. A review of graphs of the frequency change with time show that over periods of at least 6 min the rate of frequency change remained constant, while ice accumulated several wire diameters in depth. (In actual vertical profiles there is typically less than two wire diameters of ice accumulation.) The main reason there is no apparent effect of ice stiffness is that the low velocity of droplet impact upon the wire causes a soft rime ice to form. Two processes may contribute to the absence of stiffness effects. During each vibration cycle the ice is alternately under tension and compression. Generally, tension causes cracks and compression causes irreversible compression (Mellor 1983).

This situation is quite different for the Rosemount icing meter that is used at aircraft speeds, wherein ice stiffness effects are likely to be significant (Hill 1991a). Also, the amplitude of the vibrating rod of the Rosemount device is extremely small, so the effects described above do not apply.

By differentiating (4) with respect to time and using (4) to eliminate the factor $(0.2268 M_s + 0.2264 M_i)$, the result is

$$\frac{dM_i}{dt} = -\frac{2 f_0^2}{b_0 f^3}\frac{df}{dt}, \quad (5)$$

where $f_0 = f(M_i = 0)$ and $b_0 = (0.2268/0.2264)M_s = 44.366$ g cm^{-1}. The SLWC is given by

$$\mathrm{SLWC} = \frac{1}{\epsilon D w}\frac{dM_i}{dt}, \quad (6)$$

where ϵ is the collection efficiency and w is the air velocity passing the wire. By replacing dM_i/dt in (6) with (5), the result is

$$\mathrm{SLWC} = -\frac{2 f_0^2}{\epsilon b_0 D w f^3}\frac{df}{dt}. \quad (7)$$

The collection efficiency according to Langmuir and Blodgett (1946) depends upon a number of factors—that is, the drop size, the airspeed, and the wire diameter. An inertial parameter K is found from

$$K = \frac{4\rho_\omega a^2 w}{9\mu D}, \tag{8}$$

where ρ_ω is the density of liquid water (1.00 g cm^{-3}), a is the droplet radius (cm), μ is the air viscosity (1.66×10^{-4} g cm^{-1} s^{-1}), and the remaining variables have been previously defined. Another parameter, ϕ, is also used in characterizing collection efficiencies:

$$\phi = \frac{9\rho_a^2 Dw}{\mu\rho_a}. \tag{9}$$

The numerical value of ϕ for the physical conditions applicable is approximately 1.6. The difference in the collection efficiency with $\phi = 1.6$ and $\phi = 0$ is less than 0.2%. Therefore, ϕ is set to zero. The collection efficiency is found in the graph of Brun et al. (1954); in practice, the ϵ versus K curve is computerized, so that ϵ is included directly in the calculations of SLWC.

Extensive laboratory evaluation of the vibrating wire device was conducted by Hill (1989). The device was shown to yield excellent results when compared to independent measurements in a laboratory environment. In the laboratory environment a change in vibration frequency of 0.02 Hz over an interval of 1 min was readily detected. This translates to an SLWC resolution of approximately 0.01 g m^{-3}.

b. *Previous use of the vibrating wire device*

During the early usage of the vibrating wire device (prior to the present configuration of the duct housing), the wire was mounted in the humidity duct of a VIZ-type radiosonde used during the 1970s and 1980s as illustrated by Hill (1989). Measurements in both Utah orographic clouds and Great Lakes clouds resulted in an underestimation of SLWC by a factor of around 3 or 4; this indication was found by comparisons with a dual-frequency microwave radiometer.

(It is noted that at that time no published verification of microwave radiometers had yet been made. This author recognized the large differences between the quantitative results of the two SLW measuring systems. Consequently, previous publications utilize only the altitude of SLW or other indices, but not quantitative values of SLW.)

Analysis of wind tunnel measurements and visual observations of the radiosonde shortly after release into the air established that the orientation of the radiosonde of the type used at that time strongly affected the airflow through the humidity duct (Hill 1990). It was concluded that the airflow in the immediate vicinity of the vibrating wire had been greatly reduced as a result of the balloon swinging as it ascended. On the other hand, when SLW was detected it invariably occurred in the expected locations—that is, at temperatures below 0°C and with the measured relative humidity exceeding 90%. In addition, whenever there was an absence of SLW according to the radiometer the same result was found with the vibrating wire.

The altitudes of SLW maxima in various layers of SLW were measured simultaneously during January and February 1990 at Muskegon, Michigan, by the balloon-borne vibrating wire device and by a Rosemount icing meter calibrated at the National Research Council facility in Ottawa. The results are shown in Fig. 2. While these measurements were found to underestimate the quantity of SLW by a substantial amount, it is clear that the vibrating wire measured correctly the occurrence and height of SLW.

c. *Present configuration*

The configuration of the instrument as presented herein has been developed to achieve the correct airflow (equal to the balloon ascent rate) as well as to accommodate radiosondes currently in use. The VIZ radiosondes currently in use have a humidity duct that is not accessible for mounting the vibrating wire. Furthermore, in view of the previous problems it is preferable to amount the wire sensor in a separate duct that will be unaffected by the specific type of radiosonde utilized.

A special duct was designed so that an airflow speed would remain equal to the rise rate of the balloon even when the radiosonde is swinging. The resulting design is shown in Figs. 3 and 4. The design is based upon measurements made in the low-speed wind tunnel at the University of Colorado, Boulder. The dimensions

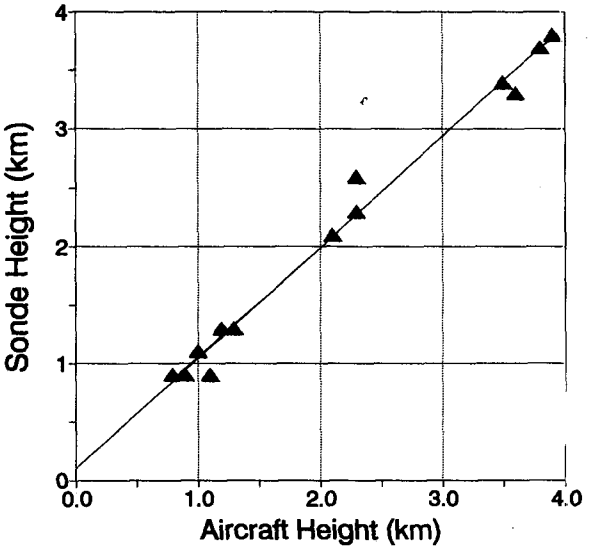

FIG. 2. Heights (km) of maximum SLW for sonde data (1984–1990 configuration) vs aircraft data at Muskegon, Michigan.

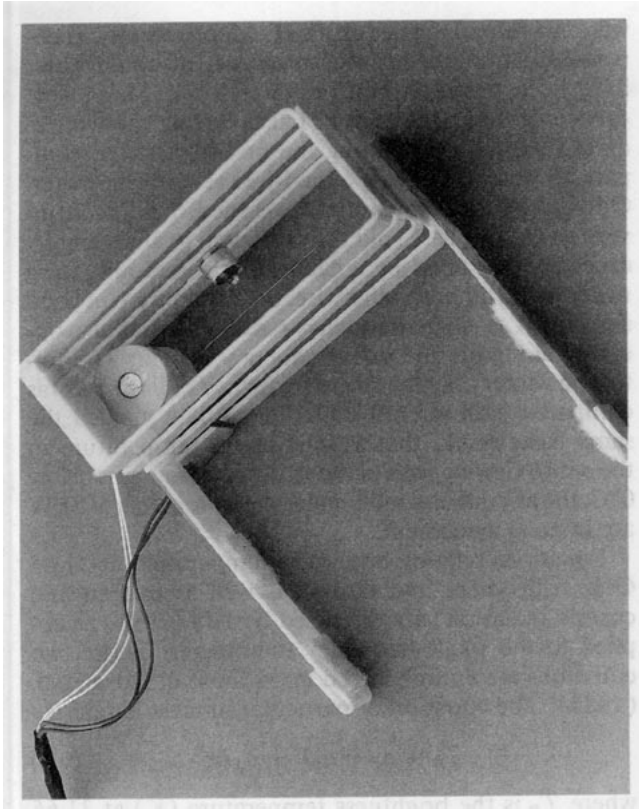

FIG. 3. Top view of the vibrating wire device.

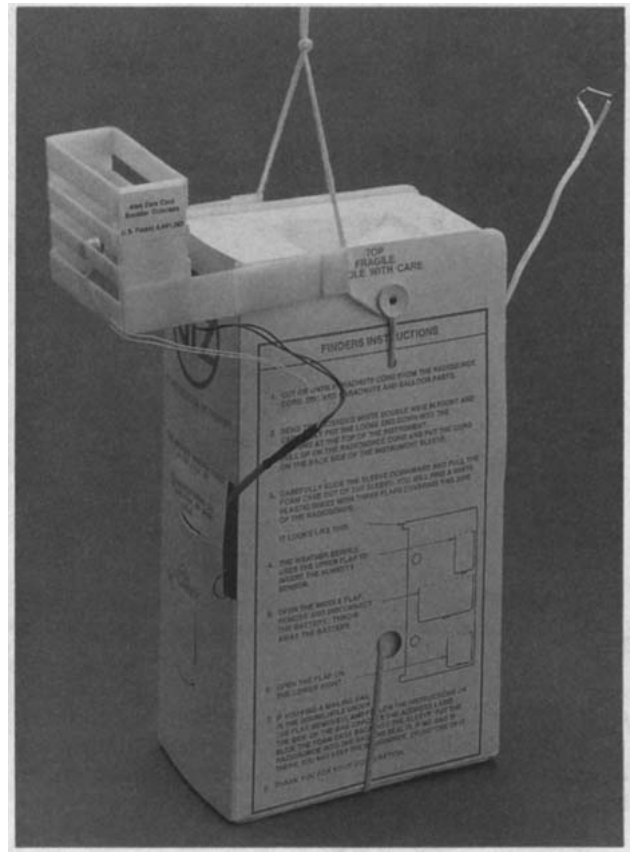

FIG. 4. View of the vibrating wire device mounted on a VIZ radiosonde.

of the duct are 3.5-cm width, 11.2-cm length, and 8.0-cm height. The wire sensor is located 3.4 cm from the bottom of the duct centered along its length.

When the wire is vibrating there is a total displacement of about 2–3 cm at the free end of the wire. While the wire vibrates generally in an up–down direction as the radiosonde ascends, the direction of vibration varies as much as 30°; individual units and motion of the duct during swinging affect the specific direction of vibration. Therefore, the airflow must remain essentially uniform in the general vicinity of the wire rather than just where the wire is located at rest.

To achieve the desired airflow pattern, a special feature of the duct is that there are three horizontal slots, or openings, along the length of the duct. When air approaches from directions other than directly into the top of the duct, the airflow remains very close to the amount measured had the air approached directly into the top of the duct, even for approach angles as much as 60° off from that direction. The added velocity due to swinging is thereby eliminated. The airflow within a solid-walled duct is shown in Fig. 5 for the case where the ambient flow is at an angle of 45° with respect to the duct opening. The component of ambient flow aligned with the duct itself is 5.8 m s^{-1}.

The airflow through the specialized duct is shown in Fig. 6 for several angles of incidence. The airflow angle is 0° when the total airflow is aligned with the

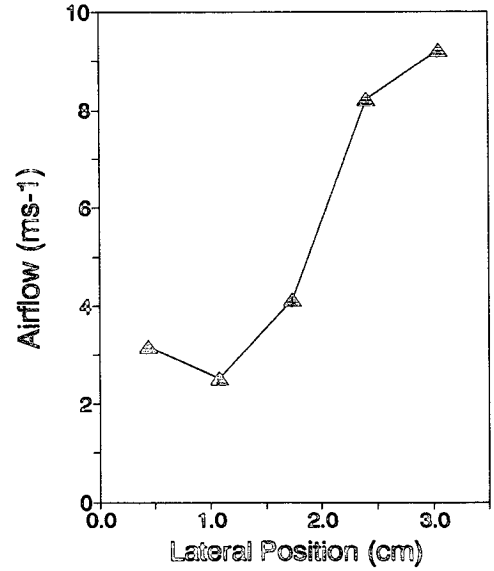

FIG. 5. Airflow through a solid wall duct tilted 45° toward the direction of airflow versus the distance across the duct.

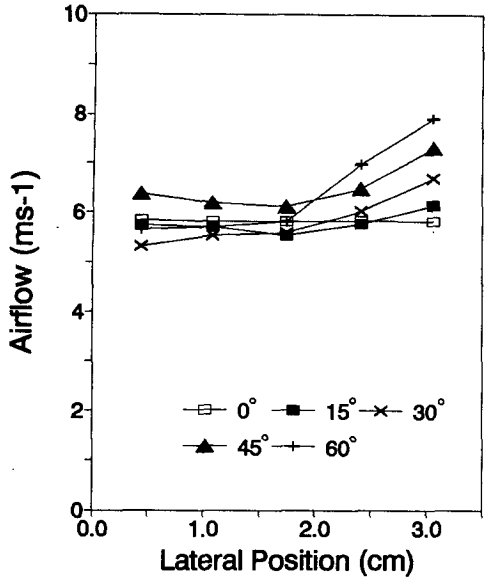

FIG. 6. Same as Fig. 3 except the duct is the new design with three horizontal openings on the long sides of the duct.

duct; the airflow angles for other airflow orientations relative to the duct are indicated on the figure. In all cases the total airflow is such that the component of ambient flow aligned with the duct is 5.8 m s^{-1}. The primary interest is the airflow at the position of the wire—that is, at d = 1.75 cm. However, the presence of a strong gradient in airflow, such as that found in Fig. 5 is not desirable. With varied airflow angles associated with balloon swinging, the effect of strong gradients within the duct is unknown. With the modified duct, the airflow through the duct remains very close to the 5.8 m s^{-1} regardless of the airflow angle. In addition, the airflow gradient near the wire remains small.

3. Radiometer

In this study a ground-based passive microwave radiometer was used to measure path-integrated liquid. The radiometer used is a single-frequency system operating at 31.65 GHz. This system is described in detail by Hill (1991b). In that study a comparison of liquid water measured by the single-frequency radiometer was found to be in good agreement with a dual-frequency radiometer. The single-frequency radiometer operates in a similar way as the NOAA Wave Propagation Laboratory dual-frequency system except that the vapor is estimated independently; also the horn antenna views directly skyward through a small Teflon window that is kept clear of ice and snow by periodic blasts of air. The calibration is done by viewing the sky during clear conditions and a reference maintained at 25°C. The latter reference is made every 10 min.

Independent comparisons of radiometric measurements with total vapor derived from radiosonde data were made by Hogg et al. 1983. More recently, independent simultaneous measurements of liquid water have been made by Hill (1991c, 1992). These were carried out along the Great Lakes during the winters of 1989 and 1990. During the first winter, the comparison was made using a dual-frequency radiometer. Only when the temperature exceeded 0°C in an inversion (in one case) did the radiometer values greatly exceed those found by a calibrated Rosemount icing meter on an aircraft; otherwise, the values were in good agreement. A single-frequency radiometer was also operated alongside the dual-frequency system. The following winter only the single-frequency radiometer was compared with aircraft data. These data yielded the same basic result, that as long as the temperature in the entire viewing path of the radiometer remains below 0°C, the aircraft and radiometer measurements of SLW are in good agreement.

Equations relating brightness temperature at 31.65 GHz with vapor and liquid (as well as oxygen and cosmic radiation) are discussed by Hill (1991) as applied to the single-frequency radiometer. Those two equations are entirely based upon those of Hogg et al. (1983). The equation of particular interest herein is

$$T_B = a_1 + a_2 V + a_3 L, \tag{10}$$

where T_B is the brightness temperature (K) at 31.65 GHz, and V and L are the path-integrated vapor and liquid (cm), respectively. The constants are a_1 = 8.24 K, a_2 = 4.761°C cm^{-1}, and a_3 = 561.5°C cm^{-1}. In a cloudless sky when L equals zero, the brightness temperature is readily found if the vapor content is known. This value of brightness temperature is treated herein as a base value. Changes from this base value are written as

$$\Delta T_B = a_2 \Delta V + a_3 \Delta L. \tag{11}$$

In fact if it is considered that the vapor remains unchanged, and the base value of the liquid is zero, then ΔT_B is written as

$$\Delta T_B = T_{BL} = a_3 L, \tag{12}$$

where T_{BL} is the brightness temperature of the liquid. Note that in this equation there is a simple linear relation between T_{BL} and L. However, in a more precise relationship there is a slight departure from this linearity. It is also noted that with the two-frequency system, the brightness temperatures at each of the two frequencies include the effect of vapor, liquid, oxygen, and cosmic radiation. This, of course, is true for the single-frequency system. The difference is that in the single-frequency system only the departures from a baseline value are used to measure liquid.

In the following discussion a reexamination of the governing equations is made, so that the effects of the cloud radiation temperature and the nonlinearity discussed above are taken into account. This approach

represents a departure from the statistical retrieval method used by Hogg et al. (1983) and others. While the microwave measurements of liquid may be best obtained over a wide range of conditions using the statistical retrieval method, it may not be the case for the present purpose of detailed comparisons with another type of instrumentation. The reason for this revised approach is that there appears to be a substantial effect of cloud radiation temperature upon the absorption of microwave radiation at the frequency of interest.

According to Snider et al. (1980), at a wavelength of $\lambda = 1$ cm, values of the absorption coefficient for temperatures of 273.16 and 265.16 K are 0.73 and 0.95 dB km^{-1} g^{-1} m^3, respectively. With a reduction in temperature of 8 K, the absorption increases by 23%. The effect on the amount of liquid is of a similar magnitude because there is an approximately (inverse) linear relationship between absorption and liquid, especially for small changes in brightness temperature. The amount of liquid at a temperature of 253 K will be about half the amount of liquid at 273 K, given the same value of measured absorption. In view of these considerations, a detailed examination of this problem is made herein.

According to Staelin (1966), water clouds absorb microwave radiation approximately as

$$\alpha_s = \frac{h_1 \mathcal{L} 10^{-h_2 T_{RL}}}{\lambda^2} \quad (\text{Np cm}^{-1}), \tag{13}$$

where α_s is the absorption (Np cm^{-1}), $\mathcal{L}$ is the liquid water concentration (g cm^{-3}), T_{RL} is the cloud temperature, and λ is the wavelength (cm). The constants are $h_1 = 3550$ g^{-1} cm^4 and $h_2 = 0.01220$ K^{-1}. The path-integrated absorption is expressed in terms of an equivalent depth of liquid water, L (cm),

$$a = \frac{h_1 L \rho_w 10^{-h_2 T_{RL}}}{\lambda^2} \quad (\text{Np}), \tag{14}$$

where ρ_w is the density of water.

An equation for absorption by liquid (e.g., Snider et al. 1980) is written as

$$T_{BL} = T_{RL}(1 - e^{-a}). \tag{15}$$

This expression is rewritten as

$$a = -\ln\left(\frac{T_{RL} - T_{BL}}{T_{RL}}\right) \quad (\text{Np}). \tag{16}$$

By use of (14) and (16), a is eliminated, so that L is a function of T_{BL} and T_{RL}; that is,

$$-\ln\left(\frac{T_{RL} - T_{BL}}{T_{RL}}\right) = \frac{h_1 L \rho_w 10^{-h_2 T_{RL}}}{\lambda^2}. \tag{17}$$

Although T_{RL} appears as a term within the logarithm, the primary effect of variations in T_{RL} is from the absorption as given in (14).

For convenience, T_{BL} is written in a similar form as in (12) expressed as

$$T_{BL} = C_L L, \tag{18}$$

where C_L (°C cm^{-1}) is a function of both T_{BL} and T_{RL}. The expression for C_L is found by eliminating L from (17) and (18). Thus,

$$C_L = \frac{T_{BL} h_1 \rho_w 10^{-h_2 T_{RL}}}{-\ln[(T_{RL} - T_{BL})/T_{RL}]}. \tag{19}$$

In Fig. 7 values of C_L are shown as a function of T_{BL} and T_{RL}. For a particular value of $C_L = 561.5$ (°C cm^{-1}), as in Eq. (12), the corresponding value of T_{RL} for small T_{BL} is approximately 268 K. This temperature corresponds closely to a statistical value used in the Hogg et al. (1983) retrieval method. By contrast, with the method used herein, an approximation of the actual liquid temperature can be utilized to obtained improved accuracy. The liquid temperature is found from the combined temperature and SLW measurements by the sondes. The specific T_{RL} is taken to be the mean of the liquid temperature weighted by the amount of liquid. In practice, L is found from (18) and (19) after T_{BL} is measured by the radiometer and T_{RL} is found from the SLW sounding by the vibrating wire.

It is evident from Fig. 7 that the coefficient C_L varies by a factor of 2 (or half) over an extreme temperature range from 273 to 243 K. More typically, with the SLW temperature in the range between about −18°C and 0°C, the coefficient C_L varies up to a factor of about 1.5. Consequently, it is important to take into account the cloud radiation temperature when using a microwave radiometer for measuring SLW, especially if comparison with another type of instrument is being made.

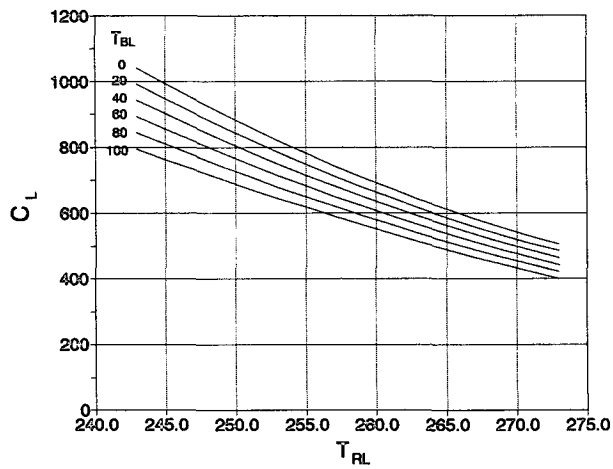

FIG. 7. Coefficient C_L versus T_{RL} and T_{BL}.

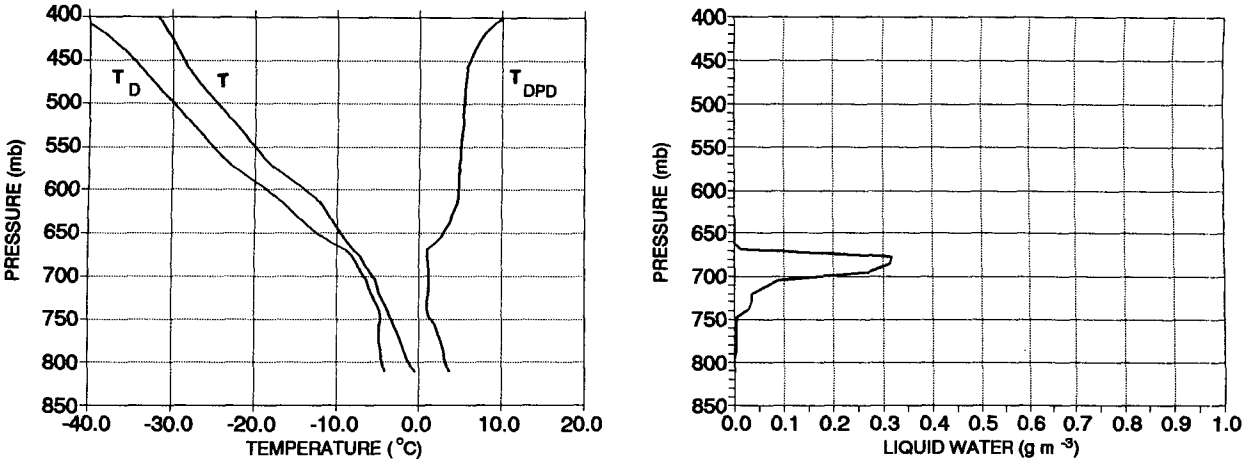

FIG. 8. Vertical profile of SLW, temperature T, dewpoint T_D, and dewpoint depression T_{DPD} for 1515 GMT 11 April 1991.

4. Comparison of vibrating wire and radiometer SLW

The vibrating wire system as described in section 2 was operated along with the single-frequency microwave radiometer during four periods: 15 March–15 April 1991, 15 March–15 April 1992, 20 November–20 December 1992, and 15 January–15 February 1993 at Boulder, Colorado. An operational requirement was that the temperature at the surface be below 0°C at the time of the radiosonde release. In the absence of a temperature restriction many more cases with SLW likely present would have been possible during these operational periods. An additional requirement was made to exclude any sounding in which an inversion was present with the temperature exceeding 0°C and there were clouds at or higher than that level. No such inversion cases were found in this study. There were many instances where the presence of SLW was probable, but it could not be ascertained whether all of the observed liquid by the radiometer was supercooled. In many cases it was evident that rain, melting, or wet snow dominated the measurement. As a result of the foregoing operational requirements, 18 valid cases were obtained. Two soundings were made during the operational periods when the surface temperature was above 0°C and precipitation was occurring at the time or within a few minutes of the balloon release. Consequently, these cases are not included in the analysis.

In future studies wherein measurements of SLW are made without the temperature restriction, the collection of sounding data will be much more rapid than in the present case. Furthermore, it will be of considerable interest to document in various meteorological conditions the portion of liquid water measured by a radiometer that can be attributed to SLW.

During ascent of the SLW device, a reduction in vibration frequency occurs when SLW is present. This reduction in frequency is the result of SLW collected on the wire as rime ice. When the sonde emerges from the top of the cloud, the relative humidity often falls sharply. At this time ice begins to sublimate from the wire and the vibration frequency increases. This pattern is quite typical. If the humidity does not fall much below ice saturation, the frequency recovery might not occur. However, in most cases observed over the past several years, SLW has been found to be associated with clouds having distinct tops and dry air above.

Sample profiles of SLW as a function of pressure are shown in Figs. 8–11 for the four cases with the largest amount of SLW. The droplet size used for the illustrated profiles is assumed to be 15 μm. The airflow at the wire [w in Eq. (6)] is taken to be the average balloon rise rate between the surface and 600 mb. The temperature, dewpoint, and dewpoint depression profiles are shown as well.

In Figs. 8 and 9 the profiles are shown for 11 April 1991 at 1515 and 1606 UTC, respectively. The maximum SLW at 1515 UTC is found at about 680 mb, whereas at 1606 UTC there are two maxima, one at 710 mb, the other at about 740 mb. The upper maximum appears to be the same layer as previous, but the lower maximum appears to be a different layer, either newly formed or advected over the site. For both soundings the SLW is found where the measured relative humidity exceeds 90% and the dewpoint depression is less than about 1°C. The cloud-top temperature for these soundings was −9°C and −10°C, respectively.

In Fig. 10 the profiles are shown for 0502 UTC 4 December 1992. Here the maximum is at about 695 mb and is a very sharp one. During this sounding, continuous light snow was falling; the snow was dendrites that were not rimed. Evidently, the snow was developing in the lower portion of the cloud, from about 750 mb down to about 800 mb. At higher altitudes the SLW was well developed. Above that layer, the humidity followed an ice-saturated profile from 650 to

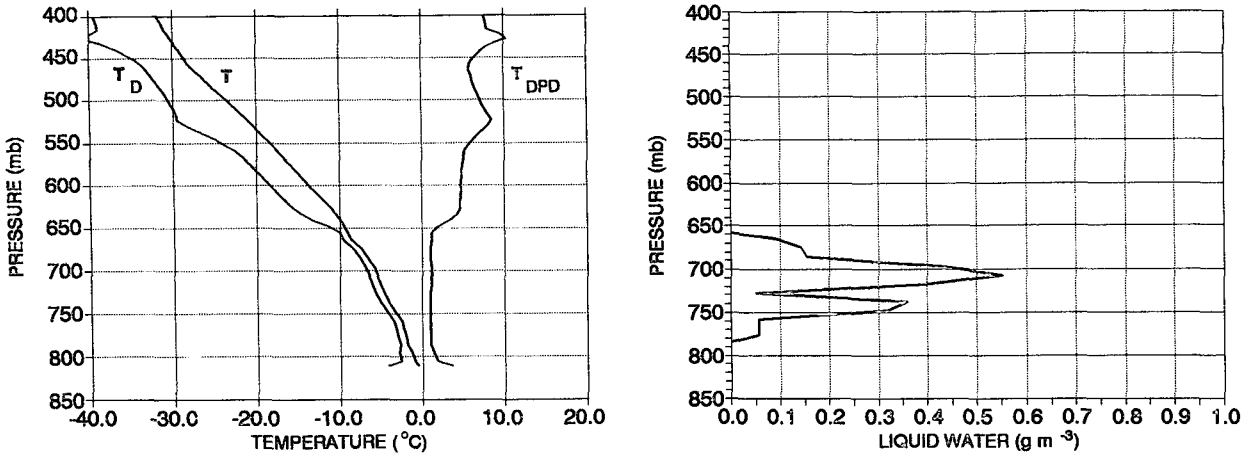

FIG. 9. Same as Fig. 9 except for 1606 UTC 11 April 1991.

550 mb, though it is not known whether ice was actually present. It is speculated that if ice were present it occurred as very small ice particles, otherwise the very high values of SLW would not likely be present below. As in the previous soundings, the SLW for this one is found where the measured relative humidity exceeds 90% and the dewpoint depression is less than about 1°C. Of considerable interest is the fact that SLW occurred in concentrations exceeding 0.5 g m^{-3} with an ambient temperature of −19°C.

In Fig. 11 the profiles are shown for 0440 UTC 11 February 1993. In this sounding there is a double maxima as in Fig. 9. The SLW is found again in the highest humidity region. In this sounding the top of the water-saturated cloud appears to be at about 560 mb; yet there is little SLW from 680 to 560 mb. At higher altitudes the humidity follows the ice saturation values.

The maximum observed SLW in each profile is a percentage of the value derived from moist-adiabatic ascent from cloud base to the height of the observed SLW maximum. For the four profiles shown, the percentages are 23%, 37%, 87%, and 43%, respectively. These are among the highest percentages of the 18 soundings. The sounding of 4 December 1992 with a value of 87% appears to be unusually high. The median value for all soundings is 20%.

It is evident from these profiles that SLW can occur in the upper, middle, or lower part of a cloud. Factors controlling the distribution of SLW at a specific location are in general the rate of production, the rate of destruction, and the transport (or advection). The production is due to lifting of water-saturated air. The destruction is due to conversion to ice or evaporation occurring during mixing with drier air. Thus, various combinations of these effects yield a variety of vertical distributions of SLW. One interesting profile that has been observed might be called a "shark's head" profile. All four of these profiles (and most others as well) tend

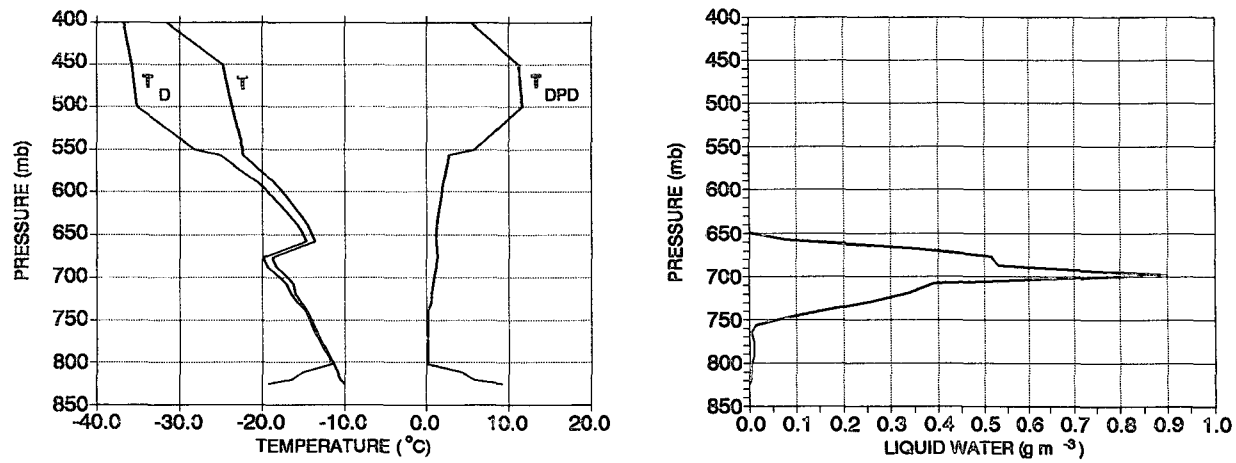

FIG. 10. Same as Fig. 9 except for 0502 UTC 4 December 1992.

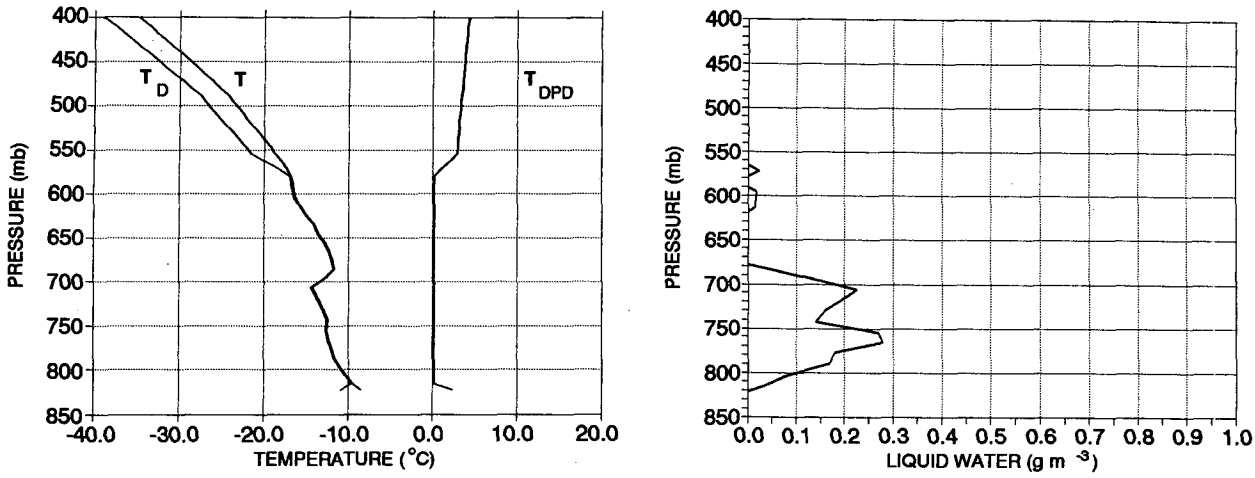

FIG. 11. Same as Fig. 9 except for 0440 UTC 11 February 1993.

to have a strong vertical gradient of SLW at the top of the SLW layer and a somewhat less strong gradient, sometimes with a local minimum as in Fig. 9, on the underside of the SLW layer.

Based upon the present study, it is found that the sensitivity of the device is approximately 0.02 g m^{-3}. This is about double the value found for laboratory data. The reason for the reduced sensitivity is that the gyration of the sonde during ascent causes a slight frequency variation. The vibration of the wire changes slightly to an elliptical mode instead of straight up and down when the orientation of the sonde is changed. This results in a slight frequency change. The measured frequency changes due to SLW must be slightly larger than otherwise to overcome this effect.

To compare the SLW measured by the vibrating wire to that of the radiometer, the SLW profile must be vertically integrated. This is done by summing from cloud base to cloud top the product of the SLW concentration in a layer and the depth of the layer. The layers are approximately 100 m. The density of the liquid is taken to be 1 g cm^{-3}.

Data for radiosonde soundings with the vibrating wire are listed in Table 1. Of the 18 soundings, 14 were at Boulder, Colorado, where the single-frequency radiometer was located, and 4 were at Stapleton Airport,

TABLE 1. Vertically integrated vibrating wire and radiometer supercooled liquid water (SLW) at Boulder (and Denver), Colorado. The sonde SLW is listed for four droplet diameters (μm), T_{RL} is the mean liquid radiation temperature, and T_{BL} is the brightness temperature of the liquid at 31.65 GHz. The vertically integrated radiometric SLW is shown for two formulations; one is based upon Eq. (12) (derived from Hogg et al. 1983) and the other is based upon Eq. (18) (derived herein). CBT and CTT are the cloud-base and cloud-top temperatures, respectively. The asterisk indicates there was a gradual transition from a dewpoint greater to less than ice saturation with increasing altitude.

Date	Time of release (UTC)	Vibrating wire (mm)				T_{RL} (K)	T_{BL} (K)	Hogg radiometer (mm)	Hill radiometer (mm)	CBT (°C)	CTT (°C)
		10 μm	15 μm	20 μm	25 μm						
30 March 1991	0045	0.113	0.098	0.093	0.091	257.6	11.1	0.198	0.154	−10	−18
30 March 1991	0230	0.116	0.104	0.099	0.097	258.1	4.5	0.079	0.062	−6	−18
11 April 1991	1515	0.139	0.123	0.118	0.116	265.7	12.4	0.220	0.211	−4	−9
11 April 1991	1606	0.339	0.303	0.291	0.285	266.9	19.5	0.346	0.345	−3	−10
12 April 1991	0352	0.023	0.020	0.019	0.019	253.6	0.0	0.000	0.000	−4	−40*
12 April 1991	0536	0.002	0.002	0.002	0.002	256.1	1.5	0.027	0.020	−2	−21*
4 December 1992	0502	0.443	0.396	0.380	0.373	255.9	23.3	0.415	0.319	−11	−22*
12 December 1992	2106	0.109	0.098	0.094	0.092	265.6	8.2	0.145	0.137	−6	−8
12 December 1992	2211	0.084	0.076	0.073	0.072	264.2	7.0	0.125	0.113	−5	−13
13 December 1992	0008	0.090	0.081	0.078	0.077	262.1	5.8	0.104	0.089	−6	−40*
13 December 1992	0852	0.128	0.116	0.111	0.110	259.8	5.0	0.090	0.073	−8	−27*
16 December 1992	0645	0.024	0.022	0.021	0.020	258.7	1.2	0.021	0.016	−5	−40*
19 December 1992	0053	0.052	0.046	0.045	0.044	263.9	3.1	0.055	0.046	−7	−13
11 February 1993	0440	0.259	0.236	0.228	0.224	260.6	13.0	0.231	0.198	−9	−18
24 February 1993	2114	0.058	0.052	0.051	0.050	266.0	5.1	0.093	0.087	−5	−8
11 March 1993	1610	0.000	0.000	0.000	0.000	265.2	1.8	0.031	0.029	−4	−14*
11 March 1993	1830	0.000	0.000	0.000	0.000	265.2	0.8	0.014	0.015	−7	−13*
12 March 1993	0152	0.155	0.139	0.133	0.131	254.9	9.6	0.171	0.125	−6	−22*

Denver, Colorado, where a National Center for Atmospheric Research (NCAR) dual-frequency radiometer of the NOAA Wave Propagation Laboratory design was located. These four cases are the last four listed in Table 1. Four droplet sizes were used to find the SLWC from the vibrating wire device: 10, 15, 20, and 25 μm. The effect of the droplet size in the SLWC calculation is most pronounced at the smaller sizes; at droplets larger than 25 μm the effect becomes negligible.

Comparisons of SLW measured by the two systems are shown in Figs. 12 and 13 for the Hogg and Hill formulations, respectively. A droplet size of 15 μm was assumed in these comparisons. The correlation coefficient for the vibrating wire and radiometer values of SLW is 0.95 for the Hogg data and 0.92 for the Hill data; the slope of the regression line is 0.89 for the former and 0.99 for the latter. These measurements are in good agreement, particularly when variations in the cloud radiation temperature are taken into account.

The variability of the sounding measurement with respect to that of the microwave radiometer may be attributed to one or more of several items: 1) in these comparisons the measurements of SLW are made over different paths, vertical for the radiometer and a balloon path for the vibrating wire; 2) the effect of the drop size on the collection efficiency of the vibrating wire is a few percent (see Table 1) at drop sizes exceeding 10 μm; 3) there exist differences in the cloud radiation temperature from case to case as taken into account in this article; and 4) there may be loss of liquid water on the wire by shedding prior to freezing.

The last of these items may produce systematic differences in results especially at warmer temperatures with large SLW droplets. In these conditions the portion of droplets freezing on the wire (freezing fraction) may be less than unity. The vigorous vibration of the wire may contribute to a reduction in the freezing fraction. Further investigation is required to determine the freezing fraction as a function of temperature, drop size, and instrument characteristics.

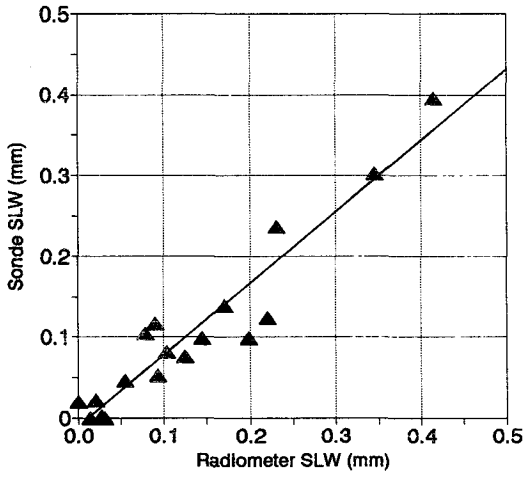

FIG. 12. Comparison of vertically integrated SLW measured by the vibrating wire device versus radiometer measured values using formulations derived by Hogg et al. (1983).

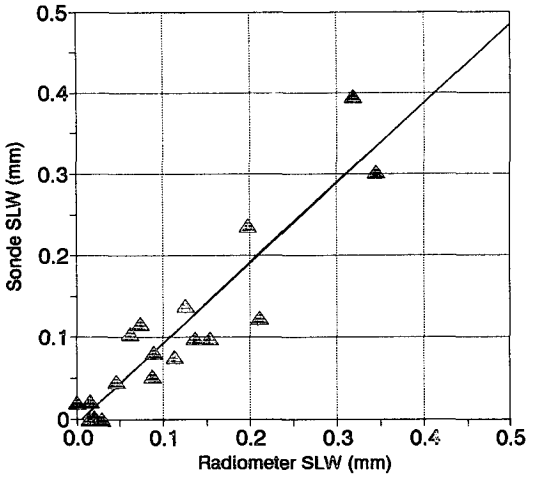

FIG. 13. Same as Fig. 12 except radiometer formulations derived herein take into account the cloud radiation temperature.

The results obtained in the present study show that there is good agreement between the path-integrated SLW of the two instruments. The primary strengths of the vibrating wire device are that SLW is specifically identified and vertical profiles are obtained. It is noted that the microwave radiometer and the vibrating wire have both advantages and disadvantages. The radiometer is advantageous in that it provides remotely operated temporally continuous measurements of path-integrated LWC; its disadvantage is that it cannot distinguish SLW from rain or melting snow and it does not measure the vertical distribution of liquid water.

The vibrating wire measurement of SLW is advantageous in that it provides unambiguously the vertical distribution of SLW; its disadvantage is that the measurement is not continuous. A single quasi-vertical distribution of SLW is obtained from each balloon release.

Because each of the two instruments has both advantages and disadvantages that are different, they both become potentially more useful when deployed together. When a microwave radiometer indicates the presence of liquid water, a sonde is utilized to ascertain whether the liquid is supercooled and its distribution with height. Such use of the two instruments provides a powerful tool to monitor or study the behavior of SLW.

5. Summary and conclusions

Independent measurements of SLW by balloon-borne vibrating wire sensors and a microwave radiometer are found to be in good agreement. This is particularly so when variations in the cloud radiation temperature are taken into account. A specially de-

signed duct to house the vibrating wire accommodates the currently used National Weather Service radiosondes; more importantly, the effect of balloon swinging on the airflow through the duct is minimized. On the other hand at temperatures a few degrees below 0°C, the possibility remains that some of the SLW is shed from the wire prior to freezing.

It is concluded that a microwave radiometer and balloon-borne vibrating wire device used in combination constitute a powerful system for the measurement of SLW. Further comparative measurements are desirable to confirm the results obtained herein and to investigate the conditions under which shedding of SLW may occur. Application of the combined systems will be beneficial especially for studies of cloud processes, aircraft icing, and winter weather modification.

Acknowledgments. The author expresses thanks and appreciation to the U.S. Army Cold Regions Research and Engineering Laboratory, Hanover, New Hampshire, for the basic support for this study under Contracts DACA89-84-C-0007 and DACA89-91-M-1089, and to the Utah Water Research Laboratory, Utah State University, Logan, Utah, for use of equipment. The author thanks Mr. Michael Seiler, Mr. Rex Logan, and Mr. Jon Hall for their contributions in the development of the microcontroller electronics. The author also thanks Mr. Glenn Chagnot, Mr. William Melton, and Mr. David Dickson for their assistance in the development of software for data analysis. Appreciation is expressed to Dr. Peter Freymuth, University of Colorado, for use of the wind tunnel to test the new duct.

REFERENCES

Brun, R. J., W. Lewis, P. J. Perkins, and J. S. Serafini, 1954: Impingement of cloud droplets on a cylinder and procedure for measuring liquid-water content and droplet sizes in supercooled clouds by rotating multicylinder method. NACA Report No. 1215, Washington, DC, 43 pp.

Guiraud, F. O., J. Howard, and D. C. Hogg, 1979: A dual-channel microwave radiometer for measurement of precipitable water vapor and liquid. *IEEE Trans. Geosci. Electron.*, **17,** 129–136.

Hill, G. E., 1989: Laboratory calibration of a vibrating wire device for measuring concentrations of supercooled liquid water. *J. Atmos. Oceanic Technol.*, **6,** 961–970.

——, 1990: Radiosonde supercooled liquid water detector. Atek Data Corp. Final Report, U.S. Army Cold Regions Research and Engineering Laboratory, Hanover, NH, 97 pp.

——, 1991a: Comments on "Laboratory and wind tunnel evaluations of the Rosemount icing detector." *J. Atmos. Oceanic Technol.*, **8,** 305–306.

——, 1991b: Measurements of atmospheric liquid water by a ground based single frequency microwave radiometer. *J. Atmos. Oceanic Technol.*, **8,** 685–690.

——, 1991c: Comparison of simultaneous airborne and radiometric measurements of supercooled liquid water. *J. Appl. Meteor.*, **30,** 305–306.

——, 1992: Further comparisons of simultaneous airborne and radiometric measurements of supercooled liquid water. *J. Appl. Meteor.*, **31,** 397–401.

——, and D. S. Woffinden, 1980: A balloon-borne instrument for the measurement of vertical profiles of supercooled liquid water concentration. *J. Appl. Meteor.*, **19,** 1285–1292.

Hogg, D. C., F. O. Guiraud, J. B. Snider, M. T. Decker, and E. R. Westwater, 1983: A steerable dual-channel microwave radiometer for measurement of water vapor and liquid in the troposphere. *J. Climate Appl. Meteor.*, **22,** 789–806.

King, W. D., C. T. Maher, and G. A. Hepburn, 1981: Further performance tests on the CSIRO liquid water probe. *J. Appl. Meteor.*, **20,** 195–202.

Knollenberg, R. G., 1970: The optical array: An alternative to scattering or extinction for airborne particle size determination. *J. Appl. Meteor.*, **11,** 86–103.

——, 1972: Comparative liquid water content measurements of conventional instruments with an optical array spectrometer. *J. Appl. Meteor.*, **11,** 501–508.

Langmuir, I., and K. B. Blodgett, 1946: A mathematical investigation of water droplet trajectories. Army Air Force Tech. Rep. No. 5418, 68 pp.

Mellor, M., 1983: *Mechanical Behavior of Sea Ice. CRREL Monogr.*, No. 83-1, U.S. Army Cold Regions Research and Engineering Laboratory, 105 pp.

Neel, C. B., Jr., 1955: A heated-wire liquid-water content instrument and results of initial flight tests in icing conditions. NASA Research Memo. A54123, 33 pp.

——, and C. P. Steinmetz, 1952: The calculated and measured performance characteristics of a heated-wire liquid-water content meter for measuring icing severity. NACA Tech. Note 2615, 37 pp.

Snider, J. B., H. M. Burdick, and D. C. Hogg, 1980: Cloud liquid measurement with a ground-based microwave instrument. *Radio Sci.*, **15,** 683–693.

Staelin, D. H., 1966: Measurements and interpretation of the microwave spectrum of the terrestrial atmosphere near 1-centimeter wave length. *J. Geophys. Res.*, **71,** 2875–2881.